International Journal of Advanced Engineering and Technology Research
ISSN: 3106-8677 (Print), ISSN: 3106-8685 (Online) | Vol. 4, No. 2, 2026

Frequency Estimation Methods for Aircraft Laser Velocimetry Under Complex Noise Environments

Yingrui Shi *

School of Information Science and Engineering, Qingdao Huanghai University, Qingdao, China

* **Corresponding author**: (Email: 202404331027@qdhhc.edu.cn)

Abstract: Accurate frequency estimation of Doppler-shifted signals is essential for aircraft laser velocimetry systems, which provide critical airspeed measurements for flight safety and operational control. However, received signals in practical flight environments are frequently contaminated by complex noise and may be subject to intermittent reception patterns, posing significant challenges for reliable frequency estimation. This study presents a systematic investigation of frequency estimation techniques for laser velocimetry signals under diverse operational conditions. Time-domain and frequency-domain noise analysis methods, including autocorrelation function analysis and power spectral density estimation, are employed to characterize the statistical properties of noise. The Fast Fourier Transform (FFT) method, Maximum Likelihood Estimation (MLE), and spectral estimation techniques are developed and comparatively evaluated for scenarios with both known and unknown signal parameters. For intermittent reception conditions, interpolation-based signal reconstruction methods and Bayesian estimation frameworks are proposed to address data sparsity. Experimental results, implemented through MATLAB simulations, demonstrate that the FFT method provides computationally efficient and intuitive frequency estimation suitable for real-time applications, whereas the MLE approach achieves superior accuracy at the expense of increased computational complexity. The proposed interpolation-based reconstruction method effectively handles intermittent sampling data, maintaining estimation reliability under incomplete data conditions. Sensitivity analysis reveals the influence of noise intensity and initial parameter selection on estimation performance. The findings offer a comprehensive framework for frequency estimation algorithm selection in aircraft laser velocimetry applications, balancing accuracy, robustness, and computational efficiency requirements.

Keywords: Aircraft Laser Velocimetry, Frequency Estimation, Noise Analysis, Fourier Transform, Maximum Likelihood Estimation, Intermittent Sampling.

1. Introduction

Air speed, defined as the velocity of an aircraft relative to the surrounding air mass, is a fundamental flight parameter closely linked to angle of attack and sideslip angle [1]. Accurate air speed measurement is critical for flight safety, as anomalous readings may lead to dangerous conditions such as aerodynamic stall, loss of control, or structural overload [2]. Traditional air speed measurement relies primarily on pitot-static systems, which are susceptible to icing, blockage, and calibration drift, limiting their reliability under adverse conditions. These limitations have motivated the development of alternative measurement techniques, among which laser-based approaches have emerged as particularly promising candidates for next-generation avionics.

Laser velocimetry measures air speed via Mie scattering: a fixed-frequency laser beam interacts with atmospheric aerosol particles, acquiring a Doppler frequency shift proportional to the relative air speed [3]. Coherent interference between the scattered and reference beams produces a signal containing this Doppler shift. The fundamental challenge lies in accurately estimating the Doppler frequency from the received signal, which is invariably contaminated by noise arising from atmospheric pressure fluctuations, temperature gradients, and mechanical vibrations [4].

$$x(t) = A\sin(2\pi f_0 t + \phi) + z(t) \quad (1)$$

Where denotes the signal amplitude, is the frequency to be estimated, is the phase, and encapsulates the noise. The received signal can be modeled as a noisy sinusoidal waveform, where the noise component originates from multiple physical sources including atmospheric turbulence, optical path variations, and electronic interference [4]. Effective frequency estimation therefore requires both accurate noise characterization and robust signal processing algorithms.

Frequency estimation of noisy sinusoidal signals has been extensively studied across diverse engineering domains, including radar, sonar, communications, and vibration analysis. The Fast Fourier Transform (FFT) remains the most widely adopted method owing to its computational efficiency and implementation simplicity [5]. However, FFT-based approaches suffer from inherent limitations in frequency resolution and susceptibility to spectral leakage. Maximum Likelihood Estimation (MLE) offers superior accuracy by formulating frequency estimation as an optimization problem under assumed noise distributions, though at significantly higher computational cost [6]. Autocorrelation-based methods provide an alternative that exploits signal periodicity without requiring amplitude or phase knowledge [7]. More recent advances include particle filtering techniques for sequential Bayesian estimation and the Non-Uniform Fast Fourier Transform (NFFT) for processing irregularly sampled data [8].

Despite these advances, a comprehensive framework that simultaneously addresses noise characterization, frequency estimation under varying levels of prior knowledge, and robust performance under intermittent signal reception remains lacking in the existing literature [9, 10]. This study bridges this gap by presenting a systematic investigation of frequency estimation methods for aircraft laser velocimetry

under complex noise environments. The principal contributions include: (1) a detailed noise analysis framework tailored to laser velocimetry signals; (2) comparative evaluation of multiple estimation techniques under known, partially known, and fully unknown signal parameters; (3) development of an intermittent reception strategy incorporating interpolation, NFFT, and Bayesian estimation; and (4) practical algorithm selection guidelines informed by sensitivity analysis.

2. Methodology

2.1. Signal Model and Noise Characteristics Analysis

2.1.1. Signal Model Formulation

The received signal is modeled as a sinusoidal signal contaminated by additive noise:

$$x(t) = A\sin(2\pi f_0 t + \phi) + z(t) \tag{2}$$

In Flight Cycle 1, the noiseless signal parameters are known: amplitude, frequency Hz (30 MHz), and phase. The unknown noise is characterized through time-domain and frequency-domain analysis. $A = 4 f_0 = 30 \times 10^6 \phi = 45^\circ z(t)$

2.1.2. Time-Domain Noise Analysis

Time-domain noise characteristics are evaluated through statistical measures. The mean value determines zero-mean properties indicative of symmetric distributions. The variance quantifies noise intensity and its impact on signal fidelity.

The autocorrelation function assesses temporal correlation: $R_x(\tau)$

$$R_x(\tau) = E[x(t)x(t+\tau)] \tag{3}$$

For white noise, the autocorrelation exhibits a sharp impulse at with rapid decay. Colored noise shows gradually decaying autocorrelation, informing algorithm selection.$\tau = 0$

2.1.3. Frequency-Domain Noise Analysis

Frequency-domain characteristics are analyzed via FFT: $x(t)$

$$X(f) = \int_{-\infty}^{\infty} x(t)\, e^{-j2\pi f t}\, dt \tag{4}$$

The power spectral density (PSD) examines whether noise energy is uniformly distributed (white noise) or concentrated in specific bands (colored noise).$x[n]$

The signal-to-noise ratio (SNR) quantifies relative signal strength:

$$\text{SNR} = 10 \log_{10}\left(\frac{P_{\text{signal}}}{P_{\text{noise}}}\right) \text{dB} \tag{5}$$

Where P_{signal}" and P_{noise}" denote the power of the signal and noise components, respectively.

2.2. Frequency Estimation with Known Amplitude and Phase

2.2.1. Fourier Transform Method

In Flight Cycle 2, amplitude and phase are known; frequency is estimated via FFT.$A = 2\phi = 0^\circ f_0$

The discrete-time signal $x[n]$ of length N is transformed via the FFT:

$$X[k] = \sum_{n=0}^{N-1} x[n] \cdot e^{-\frac{j2\pi kn}{N}}, \quad k = 0,1,\ldots,N-1 \tag{6}$$

The frequency axis is constructed as:

$$f[k] = \frac{k \cdot f_s}{N} \tag{7}$$

Where is the sampling frequency. The frequency is estimated from the maximum spectral magnitude: f_s

$$\hat{f}_0 = f[k_{\max}], \quad k_{\max} = \arg\max_k |X[k]| \tag{8}$$

FFT resolution, determined by, limits estimation accuracy and requires a sufficiently long observation window. $\Delta f = \frac{f_s}{N}$

2.2.2. Maximum Likelihood Estimation

MLE can achieve higher accuracy than FFT. Assuming zero-mean Gaussian noise with variance: $z(t)\sigma^2$

$$L(f, A, \phi) = \prod_{n=0}^{N-1} \frac{1}{\sqrt{2\pi\sigma^2}} \exp\left(-\frac{(x[n] - A\sin(2\pi f t_n + \phi))^2}{2\sigma^2}\right) \tag{9}$$

The estimate maximizes the likelihood, equivalent to minimizing squared errors:

$$\hat{f}_0 = \arg\min_f \sum_{n=0}^{N-1} \left(x[n] - A\sin(2\pi f t_n + \phi)\right)^2 \tag{10}$$

Optimization uses the Levenberg-Marquardt algorithm with initial guesses from FFT estimates.

2.2.3. Spectral Estimation with Multiple Window Functions

To mitigate spectral leakage, windowed spectral estimation is investigated using Hanning and Hamming windows:

$$x_w[n] = x[n] \cdot w[n] \tag{11}$$

Windowed FFT reduces side-lobe levels, enhancing true frequency identification, particularly with closely spaced components or strong noise.$w[n]$

2.3. Frequency Estimation with Unknown Amplitude and Phase

2.3.1. Autocorrelation Function Method

In Flight Cycle 3, neither amplitude nor phase is known. The autocorrelation method exploits periodicity without requiring these parameters.

The autocorrelation function is defined as:

$$R_x(\tau) = E[x(t)x(t+\tau)] \tag{12}$$

For a periodic signal with period, the autocorrelation attains its maximum at. The period is estimated from the first peak (excluding zero-lag): $T = \frac{1}{f_0}\tau = T$

$$\hat{T} = \underset{\tau>0}{arg\,max}\, R_x(\tau) \tag{13}$$

Frequency is derived as. This preserves periodicity while averaging out uncorrelated noise. $\hat{f}_0 = \frac{1}{\hat{T}}$

2.3.2. Periodogram Method

The periodogram provides spectral estimation from the autocorrelation:

$$P(f) = \int_{-\infty}^{\infty} R_x(\tau)\, e^{-j2\pi f \tau}\, d\tau \tag{14}$$

By identifying the frequency with maximum power, the signal frequency is estimated, combining noise-averaging with frequency-domain clarity.

2.3.3. Particle Filtering Method

For high-noise scenarios, a particle filtering approach is developed. This sequential Monte Carlo method represents

the posterior distribution using weighted particles (candidate frequencies), recursively updated based on agreement between predicted and observed values.

The algorithm proceeds through prediction and update steps. Particles propagate according to a dynamic model, then weights adjust based on data likelihood, converging toward the true frequency over successive iterations.

2.4. Frequency Estimation for Intermittent Reception

2.4.1. Problem Characterization

In Flight Cycle 4, reception is intermittent rather than continuous. The resulting data sparsity poses fundamental challenges for conventional methods assuming uniform, continuous sampling.

Intermittent reception is characterized by irregular intervals and data gaps. Direct application of FFT or autocorrelation yields degraded performance due to violated uniform sampling assumptions.

2.4.2. Interpolation-Based Signal Reconstruction

An interpolation-based reconstruction approach estimates missing signal values to reconstruct a uniformly sampled representation for subsequent frequency estimation.

Two interpolation techniques are investigated:

(1) Lagrangian Interpolation: Given known data points, the interpolating polynomial is: (t_i, x_i)

$$L(t) = \sum_{i=1}^{n} x_i \prod_{\substack{j=1 \\ j \neq i}}^{n} \frac{t - t_j}{t_i - t_j} \quad (15)$$

(2) Spline Interpolation: Cubic spline constructs a piecewise polynomial maintaining first and second derivative continuity at knot points.

FFT or autocorrelation methods are then applied to the reconstructed signal.

2.4.3. Non-Uniform Fast Fourier Transform

For irregular sampling where interpolation may introduce artifacts, the Non-Uniform FFT (NFFT) processes non-uniformly sampled data directly:

$$X(f) = \sum_{n=0}^{N-1} x_n \cdot e^{-j2\pi f t_n} \quad (16)$$

NFFT enables spectral analysis of irregularly sampled signals while preserving FFT's computational efficiency.t_n

2.4.4. Bayesian Estimation Framework

A Bayesian framework incorporates prior information with intermittent data via Bayes' theorem:

$$p(f_0 | \boldsymbol{x}_{\text{obs}}) \propto p(\boldsymbol{x}_{\text{obs}} | f_0) \cdot p(f_0) \quad (17)$$

The MAP estimate provides the most probable frequency value, yielding point estimates and credible intervals that quantify confidence under intermittent data.$p(f_0 | \boldsymbol{x}_{\text{obs}}) p(f_0)$

3. Results

3.1. Noise Characteristic Analysis Results

As shown in Figure 1, the noise-free signal exhibits a clean sinusoidal waveform. The noise characteristics of Flight Cycle 1 were analyzed using time-domain and frequency-domain methods in MATLAB.

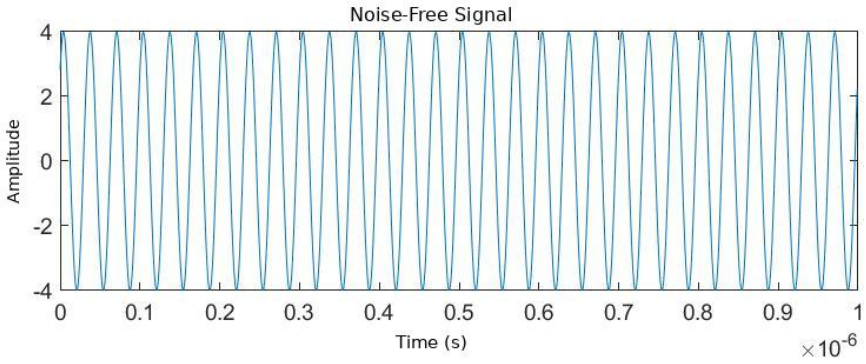


Figure 1. Time-domain waveform of the noise-free signal (Flight Cycle 1)

As shown in Figure 2, the autocorrelation function exhibited a sharp zero-lag peak with rapid decay, consistent with white Gaussian noise, indicating minimal temporal correlation.

FFT analysis revealed a clear peak at approximately 30 MHz with flat noise PSD, confirming approximately white characteristics. Minor deviations were attributed to environmental interference.

As shown in Figure 2, the noise histogram demonstrated approximately Gaussian distribution with near-zero mean, validating the AWGN assumption for MLE. The SNR provided a quantitative noise measure.

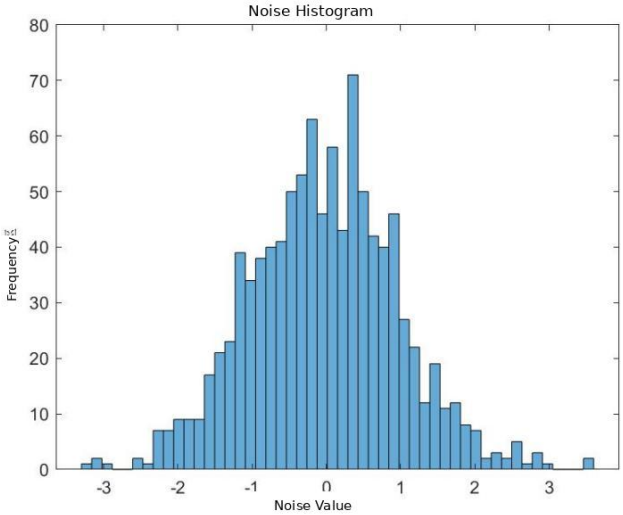


Figure 2. Histogram of the noise component (Flight Cycle 1)

3.2. Frequency Estimation Performance

3.2.1. Performance with Known Parameters (Flight Cycle 2)

As shown in Figure 3, FFT successfully identified the dominant frequency in Flight Cycle 2, with a pronounced spectral peak demonstrating effectiveness for known-parameter scenarios.

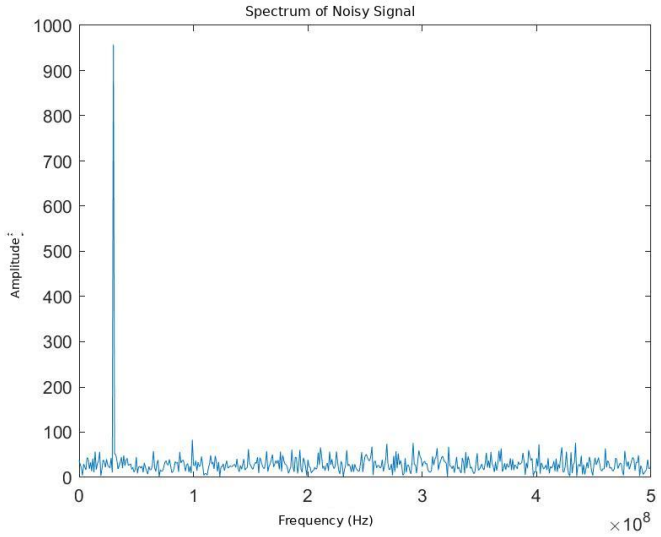


Figure 3. FFT frequency spectrum of the noisy signal (Flight Cycle 2)

MLE initialized with the FFT estimate further refined the frequency through iterative optimization, converging to a consistent value with marginally reduced error.

Comparison confirmed FFT's capability to extract the true frequency despite noise, with accuracy adequate for practical air speed measurement.

3.2.2. Performance with Unknown Parameters (Flight Cycle 3)

As shown in Figure 4, three methods were comparatively evaluated for Flight Cycle 3 with unknown parameters.

The autocorrelation method identified periodicity with clear peaks at the signal period interval. The periodogram produced consistent results. FFT identified the correct frequency directly, demonstrating robustness since it relies solely on the spectral maximum.

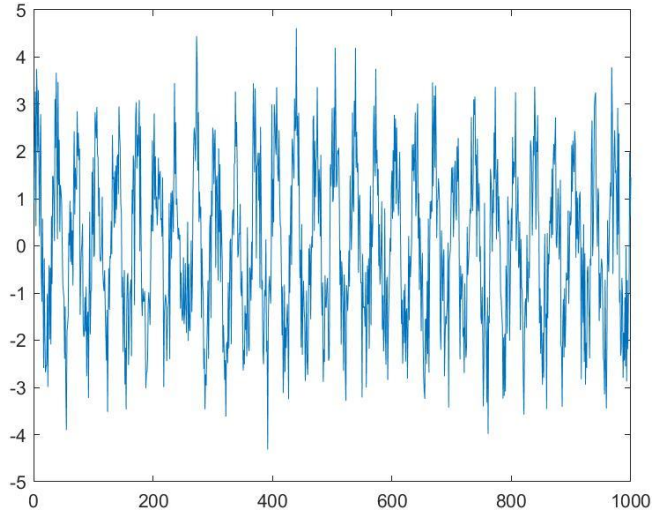


Figure 4. Time-domain waveform of the noisy signal (Flight Cycle 3)

FFT identified the correct peak directly, showing inherent robustness to amplitude and phase variations.

Particle filtering converged toward the true frequency over successive iterations, exhibiting superior robustness under high noise due to maintaining multiple hypotheses simultaneously.

3.2.3. Performance with Intermittent Reception (Flight Cycle 4)

As shown in Figure 5, interpolation-based reconstruction for Flight Cycle 4 using Lagrangian and spline methods adequately captured the sinusoidal waveform, though minor artifacts appeared near data gaps.

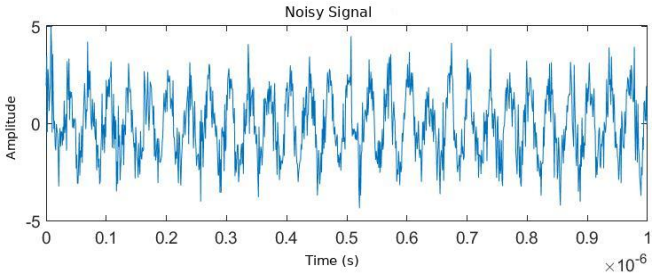


Figure 5. Signal with noise under intermittent reception (Flight Cycle 4)

Frequency estimation on reconstructed signals yielded consistent results. The NFFT method produced comparable estimates and avoids interpolation-induced artifacts.

The Bayesian framework provided posterior distributions concentrated around plausible frequencies, effectively integrating prior information with sparse data.

3.3. Sensitivity Analysis

3.3.1. Impact of Noise Intensity

Sensitivity analysis examined how noise intensity affects estimation accuracy. As noise increased and SNR decreased, error generally increased across all methods.

FFT showed particular sensitivity to high noise, where the true peak became difficult to distinguish from spurious peaks. MLE maintained greater robustness at elevated noise levels.

Autocorrelation maintained acceptable performance at moderate noise due to its noise-averaging property, but peaks attenuated at extreme levels.

3.3.2. Effect of Frequency Resolution

FFT resolution fundamentally constrains accuracy. When the true frequency falls between bins, spectral leakage causes bias, particularly problematic for closely spaced frequencies. $\Delta f = \frac{f_s}{N}$

MLE estimates frequency as a continuous parameter, avoiding this limitation. However, the optimization landscape may contain local minima, and convergence is not guaranteed with poor initial guesses.

3.3.3. Influence of Initial Parameter Selection

MLE accuracy depends critically on initial guess quality. Substantial deviation occasionally caused convergence to local optima, highlighting the importance of preliminary FFT estimates.

4. Conclusions

This study comprehensively investigated frequency estimation for aircraft laser velocimetry under complex noise and sampling conditions across four operational scenarios.

Principal findings: (1) laser velocimetry noise exhibits approximately white Gaussian characteristics; (2) FFT provides reliable estimation with known parameters; (3) autocorrelation and particle filtering effectively handle

unknown parameters; and (4) interpolation, NFFT, and Bayesian methods successfully address intermittent reception.

Algorithm selection guidance: FFT for real-time applications with moderate noise; MLE when accuracy is paramount; autocorrelation for unknown parameters; particle filtering or Bayesian approaches for intermittent reception or high-noise environments.

Future directions include multi-frequency scenarios, machine learning integration for adaptive estimation, and experimental validation with real flight data.

References

[1] Kou, J., Liu, H., Liu, Y., Liu, L., & Wan, Y. (2025). Airflow angle estimation using an observable decomposition based Schmidt Kalman filter. *IFAC-PapersOnLine*, 59(20), 1326–1331.

[2] Shao, Q., & Yang, H. (2023). How to obtain calibrated airspeed during test flight. *Large Aircraft*, (06), 61–62. (in Chinese)

[3] Zhao, J., & Liu, L. (2010). Effect of Mie scattering polarization characteristics on radiative heat exchange in plate medium. *Journal of Engineering Thermophysics*, 31(06), 1034–1036. (in Chinese)

[4] Dervieux, E., Tilquin, F., Bisiaux, A., & Uhring, W. (2024). On the accuracy of phase extraction from a known-frequency noisy sinusoidal signal. arXiv.

[5] Zuo, C., & Xu, W. (2024). Estimation of current flowmeter Doppler shift based on cyclic correlation entropy. *Acoustic Technology*, 43(04), 474–480. (in Chinese)

[6] Zhao, S. (2011). Distributed sensing system based on low coherence interference technology. Anhui University. (in Chinese)

[7] Wei, Y., Cao, M., Liu, S., et al. (2023). Study of ultrasonic wind instrument calibration period based on maximum likelihood estimation method. *China Test*, 49(S1), 186–190. (in Chinese)

[8] Li, L., Su, Z., Wu, X., et al. (2024). Zero-speed correction algorithm for pedestrian navigation with particle swarm optimization of noise parameters. *Journal of Sensing Technology*, 37(01), 42–49. (in Chinese)

[9] Naik, A. K., Nanda, S. K., Upadhyay, P. K., & Singh, A. K. (2024). Kalman-based multiple sinusoids identification from intermittently missing measurements of the superimposed signal. *International Journal of Adaptive Control and Signal Processing*, 38(9), 2996–3015.

[10] Szczepanik, R. (2026). Comprehensive review of Doppler shift localization methods: Advances, limitations, and research opportunities. arXiv.